Electronic Supplementary Material (ESI) for CrystEngComm.

Supporting Information

for the typescript entitled ”Actual and virtual structures in molecular crystals”, by Mauro Causà and Roberto Centore*

1. Discussion of the X-ray molecular structure of 4

The molecules of the studied compounds have substantially two conformational degrees of freedom: the torsion angle around the phenyl to carbonyl group (*i. e.* C5-C4-C6-N2 for **4**) indicated by ψ, and the torsion angle around the bond N-N (*i. e.* C6-N2-N3-C7 for **4**) indicated by τ. The values of the two torsion angles are gathered in Table S1 for the compounds shown in Scheme 1 of the typescript

Table S1. Selected torsion angles (°) of the studied compounds.

	NO_2[a]	**CN**[a]	**1**[a]	**2**[a]	**3**[a]	**4** at 293 K	**4** at 173 K
ψ	169.4(2)	-175.5(5)	-176.11(16)	145.9(3)	153.8(2)	-145.8(2)	-145.8(2)
τ	-85.4(2)	85.7(6)	86.5(2)	73.7(4)	95.6(2)	-70.9(2)	-67.9(2)

[a]: values are taken from ref. 1.

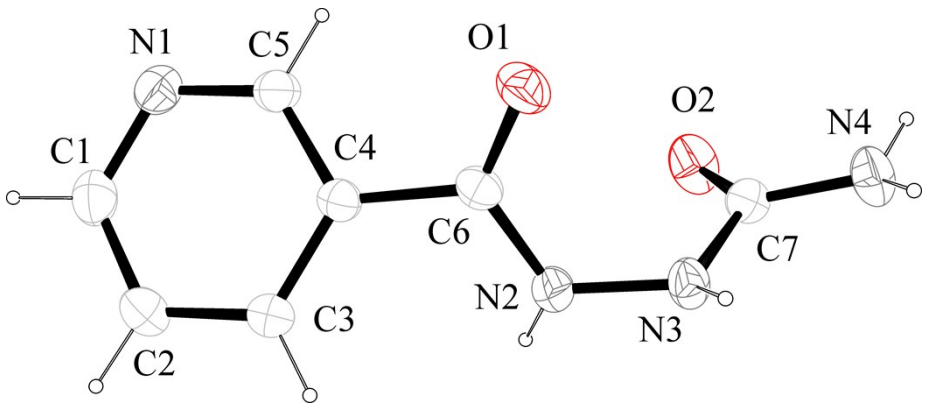

Fig. S1. Ortep drawing of the crystallographically independent molecule of **4** at 293 K. Thermal ellipsoids are drawn at 30 % probability level.

2. Geometric data of hydrogen bonds in the X-ray structure of 4

The geometric parameters of the hydrogen bond D–H···A are given in the following order: D–H (Å), H···A (Å), D···A (Å), D–H···A (°), symmetry code of the acceptor atom.

Table S2. H-bonding geometry in **4**.

	D–H···A	D–H	H···A	D···A	D–H···A	Symmetry code of A
4 at 293 K	N2–H···N1	0.92(3)	2.00(3)	2.911(3)	168(2)	2-x, 0.5+y, 1.5-z
	N3–H···O2	0.86(3)	2.11(3)	2.888(3)	150(2)	-1+x, y, z
	N4–H···O2	0.90(3)	2.07(3)	2.872(3)	148(2)	-1+x, y, z
	N4–H···O1	0.85(3)	2.11(3)	2.942(3)	167(3)	1-x, -y, 1-z
4 at 173 K	N2–H···N1	0.92(2)	1.99(2)	2.895(2)	168(2)	2-x, 0.5+y, 1.5-z
	N3–H···O2	0.84(2)	2.12(2)	2.883(2)	150(2)	-1+x, y, z
	N4–H···O2	0.89(2)	2.05(2)	2.861(3)	150(2)	-1+x, y, z
	N4–H···O1	0.89(2)	2.06(2)	2.926(2)	165(2)	1-x, -y, 1-z

3. Optimization procedure and results

Each structure was first optimized in its own packing, starting from the corresponding room temperature (RT) crystal structure (cell and fractional coordinates). In this way, the lattice energies U_{11}, U_{22}, U_{33}, U_{44}, and the corresponding lattice densities were obtained.

For the optimization of the semicarbazides in the packings of other semicarbazides, the procedure was as follows.

For the optimizations in packing type 1, the initial model was assembled starting from the RT crystal structure of **1** (cell and fractional coordinates) replacing the *p*-nitrogen atom with a C-H group and the *meta* C-H group with a nitrogen atom (U_{41}). Standard values for the bond lengths and angles were considered.

For the optimization in packing type 2, the initial model was assembled from the RT crystal structure of **2** (cell and fractional coordinates) replacing the fluorine atom by a H atom and the *meta* C-H group with a nitrogen atom (U_{42}), using standard values for the bond lengths and angles.

For the optimizations in packing type 3, the initial model was assembled from the RT crystal structure of **3** (cell and fractional coordinates) replacing the chlorine atom by a H atom and the *meta* C-H group with a nitrogen atom (U_{43}), using standard values for the bond lengths and angles. For the optimizations in packing type 4, the initial model was assembled from the RT crystal structure of **4** (cell and fractional coordinates) replacing the *meta* N atom with a C-H group and the *para* C-H with N (U_{14}), C-F (U_{24}) or C-Cl (U_{34}). Standard values for the bond lengths and angles were considered.

In Table S3 are reported the experimental cell parameters at 298 K and 173 K and the optimized cell parameters for all the semicarbazides.

Table S3. Experimental cell parameters at 298 K, 173 K and optimized cell parameters (at 0 K) for **1**, **2**, **3** and **4**.

Compound [a]	*a* (Å)	*b* (Å)	*c* (Å)	β (°)
1 (298 K)	4.513(2)	20.038(7)	9.619(5)	106.34(2)
1 (173 K)	4.515(2)	19.982(7)	9.555(5)	108.75(2)
1 opt	4.5104	19.8942	9.4009	114.64
2 (298 K)	7.785(4)	13.578(6)	8.459(4)	99.74(2)

2 173 (K)	7.746(4)	13.458(6)	8.415(4)	99.51(2)
2 opt	7.7535	13.0315	8.3428	100.87
3 (298 K)	6.786(4)	4.604(3)	30.169(8)	90.76(3)
3 (173 K)	6.733(4)	4.583(3)	30.058(6)	90.68(3)
3 opt	6.4898	4.5509	30.1063	89.31
4 (298 K)	4.587(3)	9.666(4)	19.148(5)	91.76(2)
4 (173 K)	4.580(2)	9.633(3)	19.017(5)	91.18(2)
4 opt	4.5505	9.2174	18.9881	93.43

[a] Data for **1**, **2** and **3** are taken from ref. 1.

In Table S4 we report the cell parameters for the optimized structures. Each structure is identified in the first column by a two-number code, m/n. The first number identifies the compound (Scheme 1 of the typescript, m = 1, 2, 3, 4), the second identifies the type of packing (n = 1, 2, 3, 4).

Table S4. Cell parameters for the optimized structures (at 0 K). The cell parameters of the optimized structures corresponding to the real structures (also given in Table S3) are highlighted in yellow.[a]

Structure	*a* (Å)	*b* (Å)	*c* (Å)	β (°)
1/1	4.5104	19.8942	9.4009	114.64
2/1	4.5026	19.4527	9.4888	104.70
3/1	4.5142	23.0919	9.4181	111.82
4/1	4.4521	19.4517	9.4198	111.88
1/2	7.4053	13.8431	7.8201	91.39
2/2	7.7535	13.0315	8.3428	100.87
3/2	7.7008	13.5214	8.9511	106.71
4/2	7.9112	12.7802	7.7484	105.14
1/3	6.2273	4.5987	27.4056	99.94
2/3	6.4284	4.5501	28.6564	86.73
3/3	6.4898	4.5509	30.1063	89.31
4/3	6.4846	4.5408	27.3289	87.28
1/4	4.5474	9.9853	17.3636	96.69
2/4	4.5439	9.6444	18.3194	96.43
3/4	4.5614	9.8527	19.3740	94.20
4/4	4.5505	9.2174	18.9881	93.43

[a] Data for **1**/**1**, **2**/**1, 3**/**1**, **1**/**2**, **2**/**2**, **3**/**2**, **1**/**3**, **2**/**3**, **3**/**3** are taken from ref. 1.

Considering the real structures, Table S3, the agreement between the lattice parameters of the room temperature X-ray structures and those of the optimized structures is quite good. The agreement between cell axes is within 4 % and between angles is within 8 %. The figures drop to 3 % and 5 % if the experimental lattice parameters measured at 173 K are considered. The good agreement between the experimental and optimized lattice parameters is indicative of the soundness of the

theoretical method used in the calculations and of the reliability of the estimated theoretical quantities (lattice energy, density etc.).

In the case of the virtual structures, of course we do not have any experimental datum to be compared with. However, a useful comparison can be performed between the final optimized lattice parameters of the virtual structure and the lattice parameters of the actual (experimental) structure from which the starting model is built up (*vide supra*). This is shown in Table S5.

Table S5. Variation of each optimized lattice parameter as compared with the initial model for the virtual structures. [a]

Virtual structure	$\Delta a/a$	$\Delta b/b$	$\Delta c/c$	$\Delta\beta/\beta$
2/1	-0.2 %	-3 %	-1 %	-1.5 %
3/1	0.03 %	15 %	-2 %	5 %
4/1	-1 %	-3 %	-2 %	5 %
1/2	-4 %	3 %	-7 %	-8 %
3/2	-0.6 %	0.5 %	6 %	7 %
4/2	1.6 %	-6 %	8 %	5 %
1/3	-8 %	-0.1 %	-9 %	10 %
2/3	-5 %	-1 %	-5 %	4 %
4/3	-5 %	-1 %	-5 %	-4 %
1/4	-0.9 %	3 %	-9 %	5 %
2/4	-0.9 %	-0.2 %	-4 %	5 %
3/4	-0.6 %	2 %	1 %	3 %

[a] Data for **2**/**1, 3**/**1**, **1**/**2**, **3**/**2**, **1**/**3**, **2**/**3** are taken from ref. 1.

Also in this case the changes due to the optimization procedure are rather small, that indicating that the experimental packing of a specific semicarbazide is a good starting model for the packing of every other and it is retained during the optimization. The most relevant change is observed for the *b* axis of the virtual structure 3/1. But this is clearly expected because, in the packing of type 1, the *b* axis is related with the length of the molecule and the starting model for the optimization is that of semicarbazide **1**, which has a molecular length significantly shorter than **3** (*p*-nitrogen instead of *p*-C-Cl). In summary, the data of Table S5 clearly confirm the virtual isomorphism of all the investigated semicarbazides in each of the four packings. This is also confirmed by the structural parameters ψ and τ (*vide supra*) of the optimized structures (Table S6), which keep similar values for different semicarbazides optimized in the same packing.

Table S6. Selected torsion angles (°) of the optimized structures. The optimized structures corresponding to the real structures are highlighted in yellow.[a]

Structure	ψ (°)	τ (°)
1/1	-168.61	85.62
2/1	-176.18	-92.52
3/1	167.43	-83.90
4/1	172.48	-94.79
1/2	130.97	61.52
2/2	146.60	73.34
3/2	146.15	70.90
4/2	162.42	80.49
1/3	150.81	92.27
2/3	152.09	92.84
3/3	152.51	93.28
4/3	-154.70	-89.27
1/4	-156.65	-78.37
2/4	-163.25	-77.72
3/4	-164.33	-68.77
4/4	-142.69	-67.84

[a] Data for **1**/**1**, **2**/**1, 3**/**1**, **1**/**2**, **2**/**2**, **3**/**2**, **1**/**3**, **2**/**3**, **3**/**3** are taken from ref. 1.

4. Analysis of virtual structures

4.1. Discussion of some virtual structures and estimation of the energy of intermolecular contacts

Crystal packings for the virtual structures 2/4 and 3/4 are reported in Figs. S2 and S3 respectively.

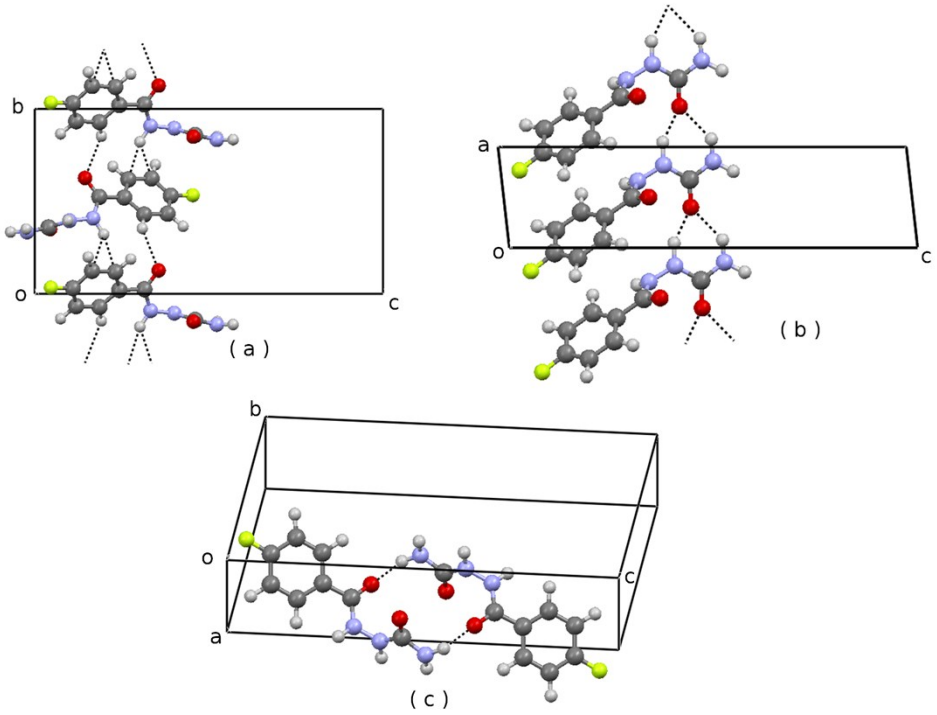

Fig. S2. Partial crystal packing of the virtual structure 2/4 (i. e. compound **2** optimized in the packing of compound **4**). (a) view down a; (b) view down b; (c) skew view.

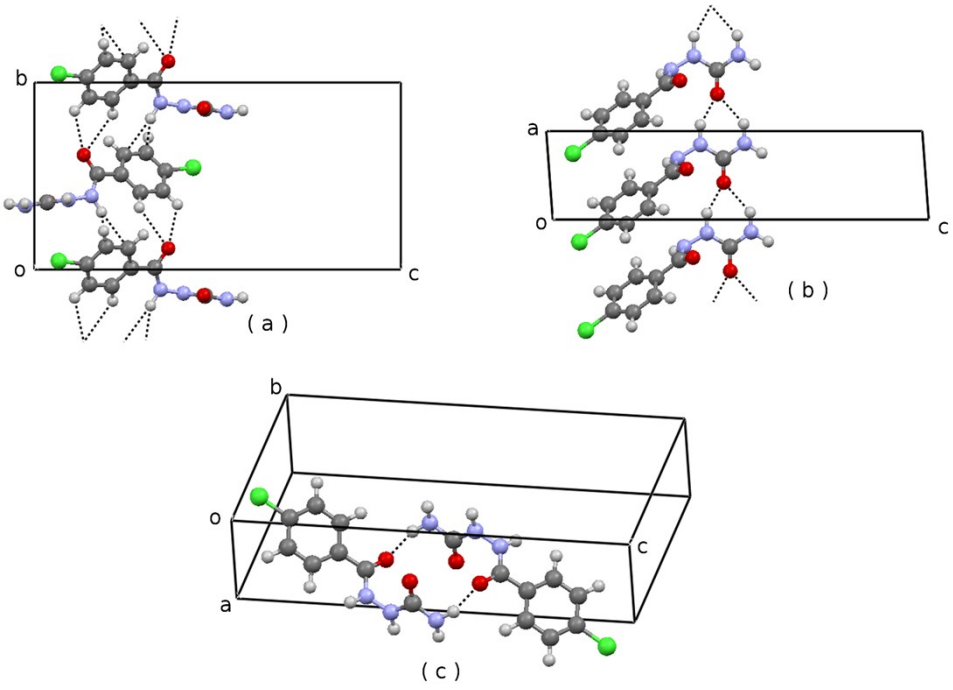

Fig. S3. Partial crystal packing of the virtual structure 3/4 (i. e. compound **3** optimized in the packing of compound **4**). (a) view down a; (b) view down b; (c) skew view.

There is a full analogy between the virtual structures 2/4 and 3/4 with the virtual structure 1/4 discussed in the typescript. In fact, also in 2/4 and 3/4 the urea chains and the centrosymmetric dimers are retained (Fig. S2(b) and (c) and Fig. S3(b) and (c)), but the H bonded chain N-H···N is not, and it is replaced by a chain held by weak N-H···π and C-H···O interactions (Fig. S2(a) and Fig. S3(a)). As a consequence, the lattice energy of 2/4 and 3/4 is about 7 kcal/mol higher than 4/4, because of the loss of the strong H bond.

The virtual structure 4/2 is shown in Fig. S4. This structure is clearly isomorphous with the actual structure 2/2, as it can be deduced by comparing the packing diagrams (Fig. S4 with Fig. 4 of ref. 1) and the unit cell parameters, reported in Tab. S4.

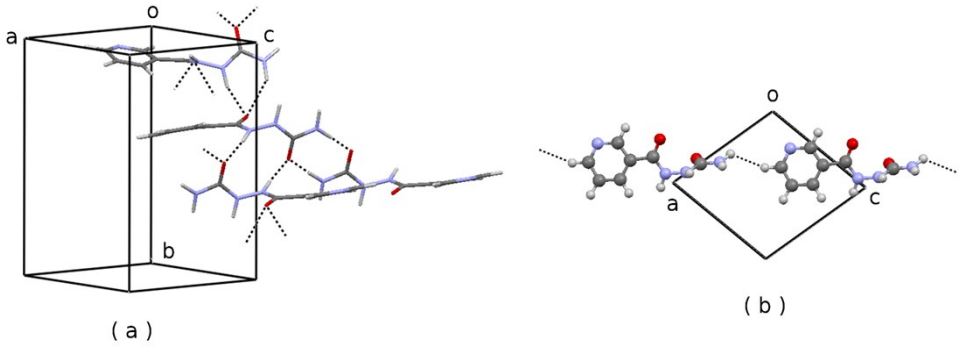

Fig. S4. Partial crystal packing of the virtual structure 4/2 (i. e. compound **4** optimized in the packing of compound **2**). (a) H-bonding patterns involving amide and urea groups; (b) a chain involving close contact between the N-H donor not involved in pattern (a) and the *para* H on the ring; the chain is generated by translation. This figure should be compared with Fig. 4 or ref. 1.

The strong H bonding patterns, shown in Fig. S4(a) for 4/2 are analogous to 2/2 so, a high difference in lattice energy is not expected between 2/2 and 4/2. In particular, in the actual structure 2/2, the chains analogous to Fig. S4(b) are formed by N-H···F contacts,[1] while in virtual 4/2 the chains feature a facing N-H···H (Fig. S4(b)). From Table 1 of the typescript, by comparing U_{22} with U_{42}, one could infer that the contact N-H···F is more stable than N-H···H by about 1.4 kcal/mol or, alternatively, that taken 0 kcal/mol the energy of the interaction N-H···H, that of the interaction N-

H···F is -1.4 kcal/mol. This is consistent with organic fluorine being a weak H bonding acceptor.[2] The H-bonding patterns of the virtual structure 4/3 are shown in Fig. S5. This structure is clearly isomorphous with the actual structure 3/3, as it can be deduced by comparing the packing diagrams (Fig. S5 with Fig. 5 of ref. 1) and the unit cell parameters, reported in Tab. S4.

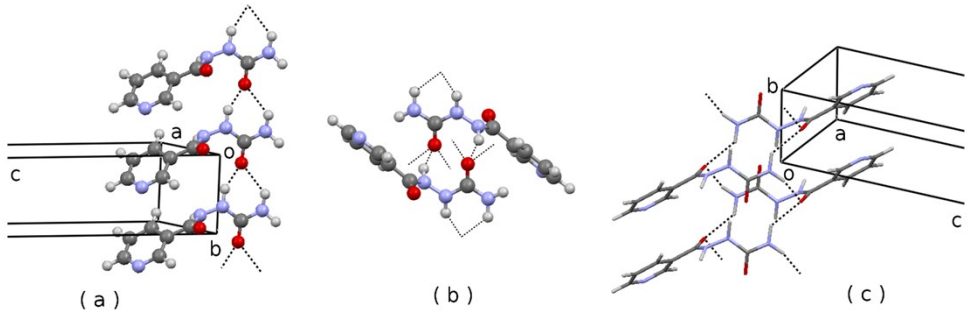

Fig. S5. H-bonding patterns in the virtual structure 4/3 (i. e. compound **4** optimized in the packing of compound **3**). (a) A urea chain; (b) a urea carbonyl as a trifurcated acceptor; and (c) an amide carbonyl as a bifurcated acceptor. This figure should be compared with Fig. 5 of ref. 1.

Lattice energy is similar in the two structures, with U_{33} being 2.2 kcal/mol lower than U_{43}. Of course, this is consistent with the fact that the strong H-bonding patterns are identical in the two structures. The difference could be tentatively related with weak C-H···Cl interactions[2] present in actual 3/3 that are replaced by weak C-H···π interactions in virtual 4/3.

4.2 Overlay of molecules in actual and virtual structures

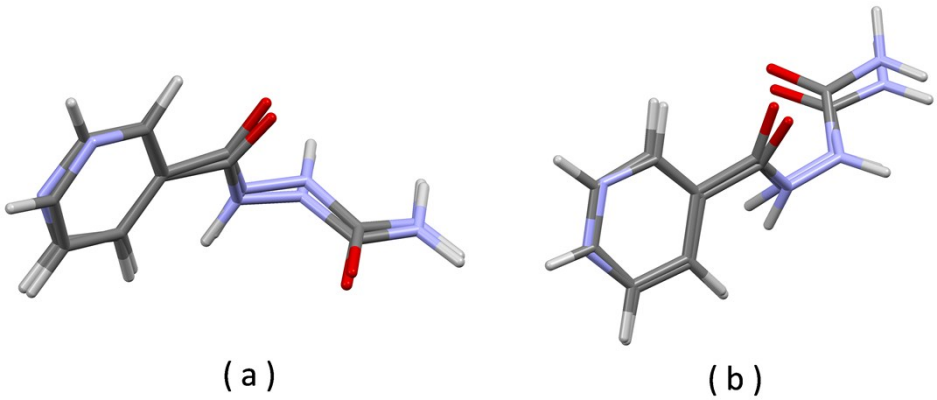

Fig. S6. Overlay of the crystallographically independent molecules in the otimized crystal structures of: (a) 4/1 and 1/1; (b) 1/4 and 4/4.

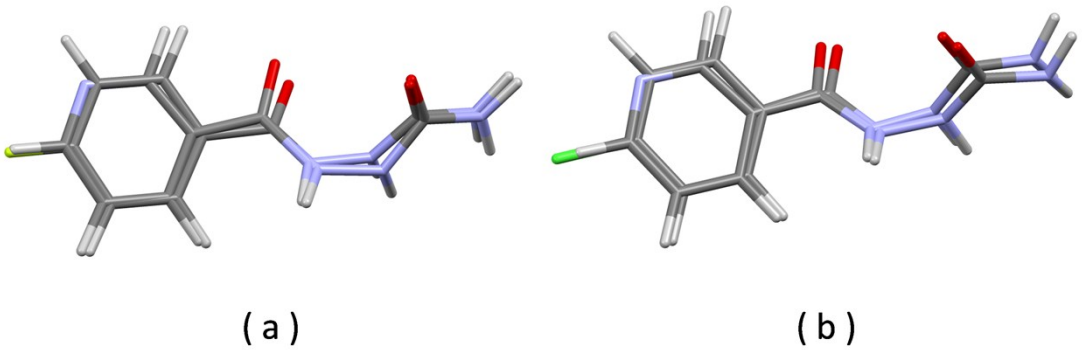

Fig. S7. Overlay of the crystallographically independent molecules in the otimized crystal structures of: (a) 4/2 and 2/2; (b) 4/3 and 3/3.

4.3 Specific results for the virtual structure 4/1

In Fig. S8 are reported different projections of the independent molecule of the virtual structure 4/1 before and after the optimization procedure.

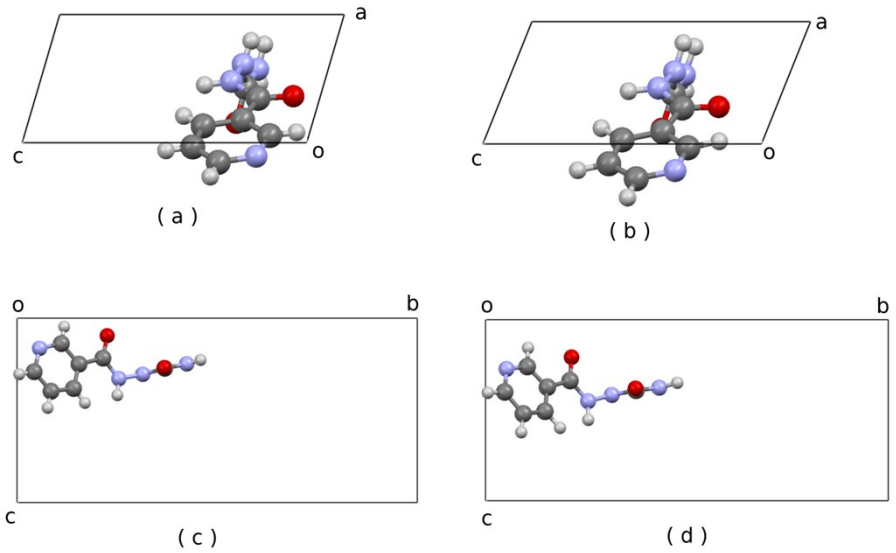

Fig. S8. Projections of the independent molecule before ((a), (c)) and after ((b), (d)) the optimization procedure, for the virtual structure 4/1.

From the different projections it is evident that, during the optimization, the independent molecule is displaced mainly along the **c** axis. In particular, by comparing the fractional z coordinates of each

atom of the molecule before and after the optimization, it results a fairly constant value $\Delta z \cong 0.11$, that corresponds to a displacement of about 1 Å.

References

[1] R. Centore, M. Causà, F. Cerciello, F. Capone, S. Fusco, *CrystEngComm*, 2014**, 16**, 9168-9175.

[2] L. Brammer, E. A. Bruton, P. Sherwood, *Cryst. Growth Des.*, 2001, **1**, 277-290.

5. Experimental and calculated powder X-ray diffraction patterns of 4

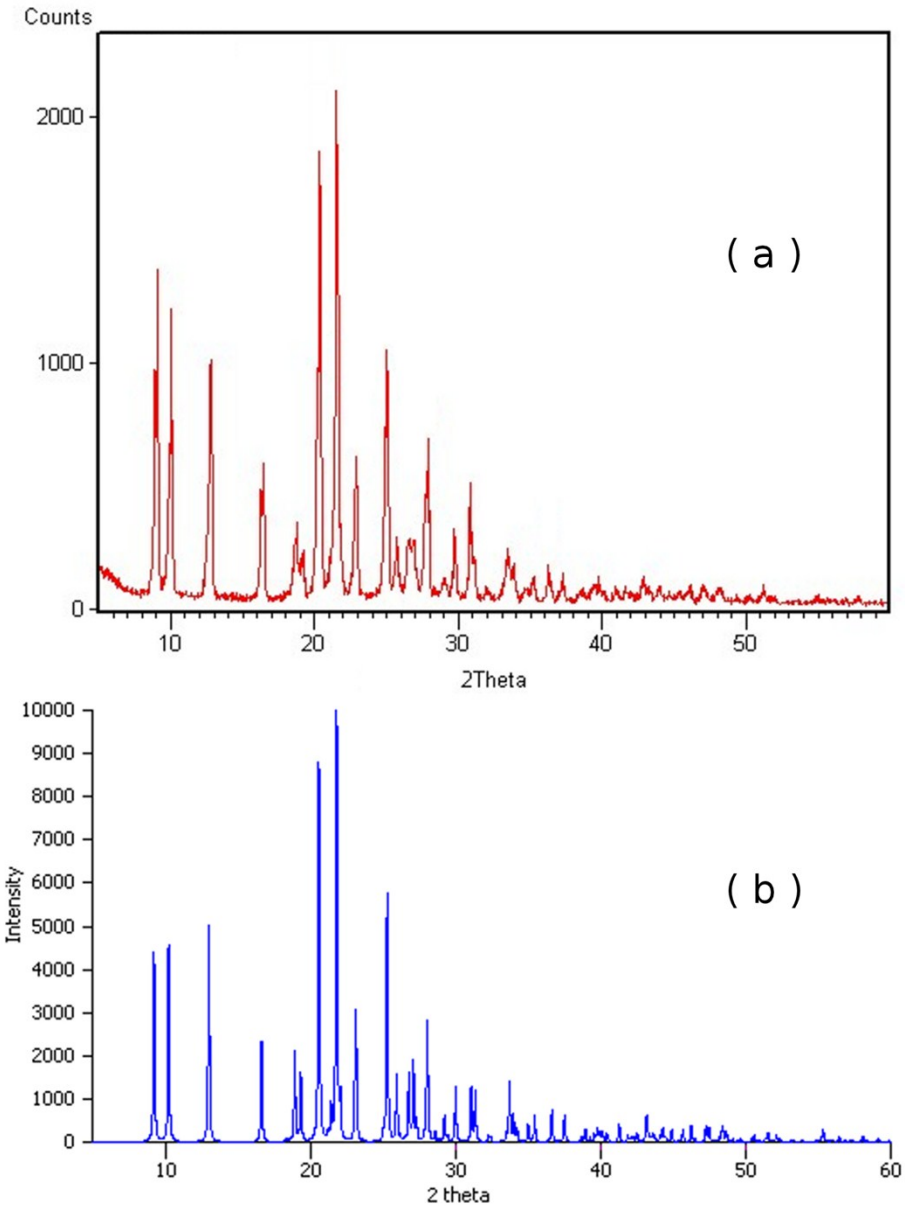

Fig. S9. (a) Experimental X-ray powder diffraction pattern of **4** recorded from the bulk sample at 293 K; (b) X-ray powder diffraction pattern of **4** calculated from the single crystal X-ray structure at 293 K. In both cases CuKα radiation was used.

The matching between the measured and calculated powder spectra is very good, and this proves that the bulk sample only contains the crystal phase described in the typescript.

6. DSC analysis of the bulk sample of 4

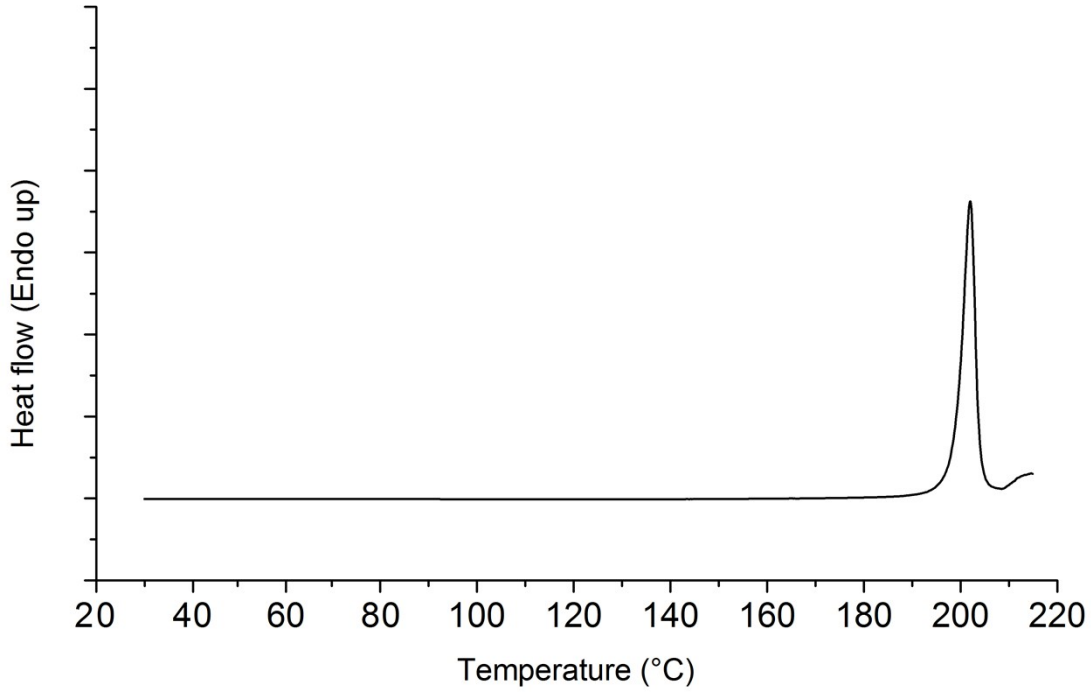

Fig. S10. DSC thermogram, on heating, of a bulk sample of **4**. Scanning rate 10 K/min.

7. NMR spectra of compound 4

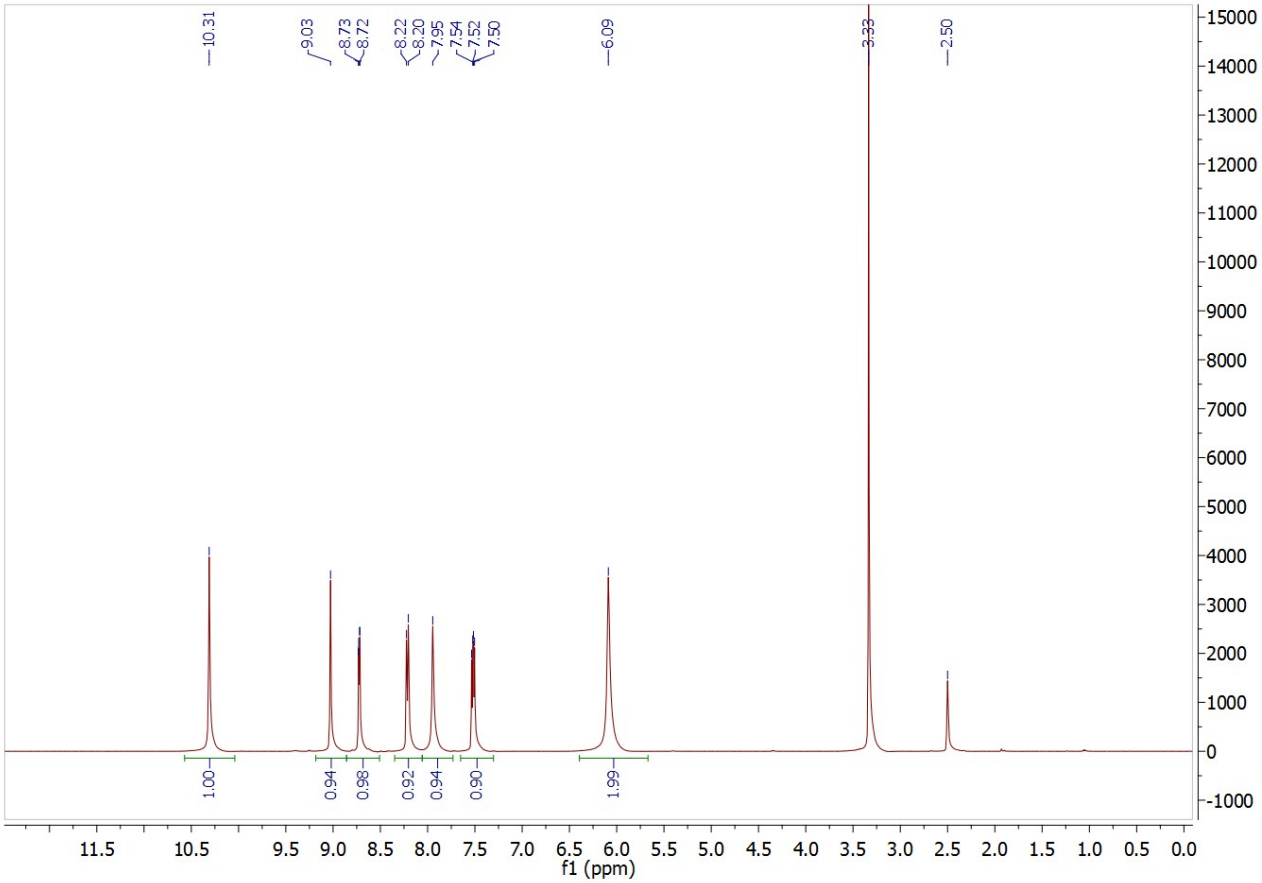

Fig. S11. 400 MHz ^{1}H-NMR spectrum of **4**. Solvent is D6-DMSO, T= 25 °C.

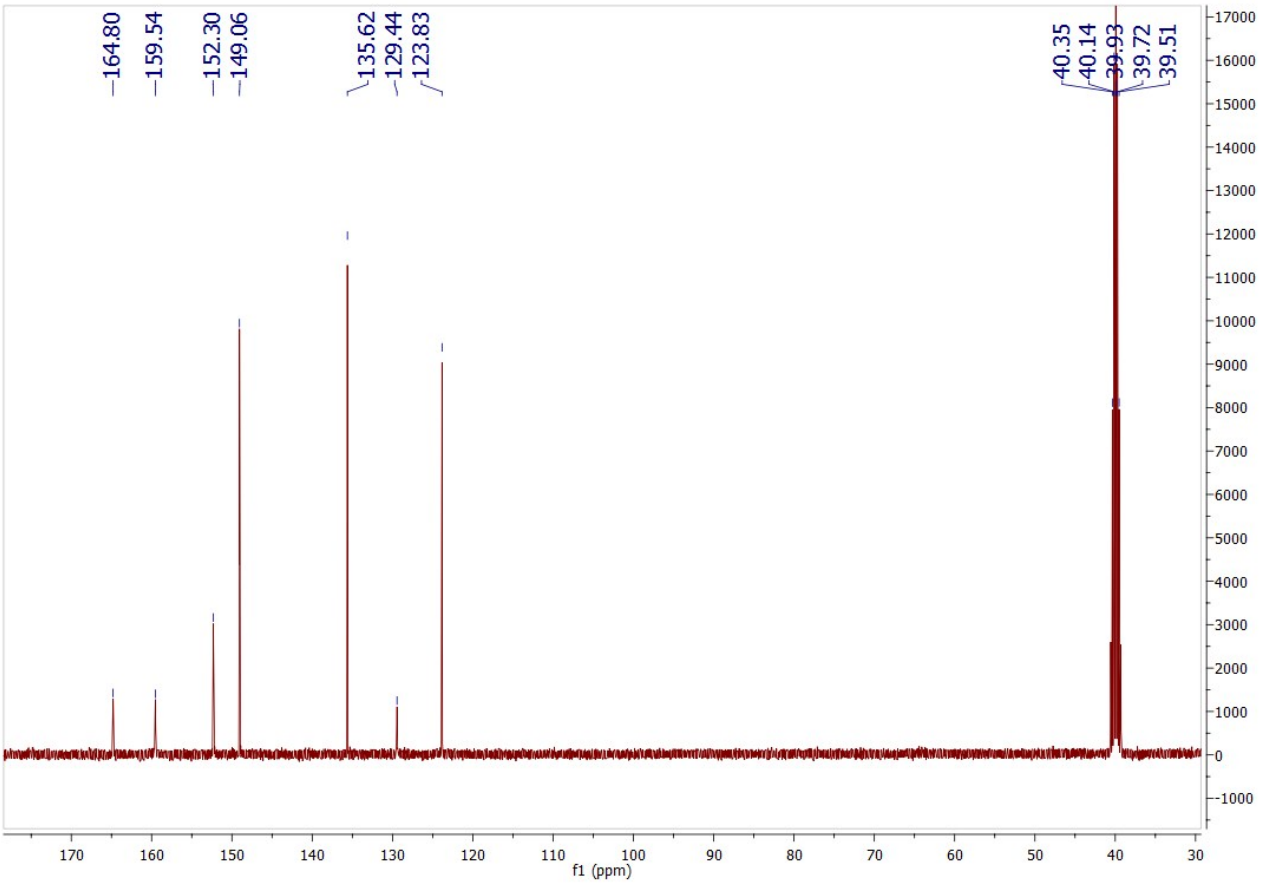

Fig. S12. ^{13}C-NMR spectrum of **4**. Solvent is D6-DMSO, T = 25 °C.